Highly Active Platinum Single-Atom Catalyst Grafted onto 3D Carbon Cloth Support for the Electrocatalytic Hydrogen Evolution Reaction

Po-Wei Yu[1], Sait Elmas[1]*, Xun Pan[1], Yanting Yin[1], Christopher T. Gibson[1,2], Gunther G. Andersson[1] and Mats R. Andersson[1]*

[1] - *Flinders Institute for Nanoscale Science & Technology, Flinders University, Bedford Park SA, Adelaide, Australia.*

2 - Flinders Microscopy and Microanalysis, College of Science and Engineering, Flinders University, Bedford Park, SA 5042, Australia

* - Corresponding authors:
Sait Elmas: sait.elmas@flinders.edu.au;
Mats Andersson: mats.andersson@flinders.edu.au

ABSTRACT

Platinum single-atom catalysts (PtSACs) on 3D support are emerging as new frontier in catalysis due to their atom-economy, outstanding performance and the advantage to bridge the gap between homogeneous and heterogeneous catalysis. Here we report on a simple, single-step electrochemical grafting attachment of a metal-selective ligand, 2,6:2',2"-terpyridine, and the synthesis of platinum single-atom electrocatalyst *via* metal uptake from aqueous salt solution. At an ultra-low loading of 0.26 ± 0.02 $\mu g \cdot cm^{-2}$ of platinum, the single atom catalysts supported on porous 3D carbon cloth electrode *via* chemical bonding revealed the highest reported mass activity of 77.1 $A \cdot g_{Pt}^{-1}$ at η = 50 mV/RHE compared to the commercial catalyst 20 % Pt/C. The electro-grafted terpyridine ligand can also act as an effective scavenger for leached platinum from the counter electrode during extended operational hours. The method to make the PtSAC is facile, non-hazardous and versatile without involving any elaborative pre- and/or post-treatment steps and, the value of the added platinum to the ligand is only 0.1 US$$\cdot m^{-2}$.

Keywords: *Single-atom catalyst, platinum, terpyridine, electro-grafting, self-supported electrodes, hydrogen evolution, electrocatalysis.*

INTRODUCTION

Hydrogen is considered the most promising and competitive energy carrier, as it is clean, renewable and available in abundance. With an energy density of 120-140 MJ/kg being three times higher than the same amount of energy gasoline can provide and the possibility to feed hydrogen gas into the existing infrastructures, the transition from fossil based fuels to the hydrogen economy has started.[1,2] Undoubtedly, when combined with renewable energy sources such as wind and solar power, hydrogen has enormous potential to become one of the main alternative energy carrier to push toward zero greenhouse gas emissions in the near future.[3–5] At present, steam reforming of methanol and ethanol is the main process in hydrogen production. However, the product of the steam reforming is not only hydrogen and water; leaving inevitably the carbon dioxide footprint behind, the question remains as to whether steam-reforming of hydrocarbons can still be defined as "clean". Moreover, the steam reforming process requires high temperature and separation methods making hydrogen as energy carrier also less profitable.[6–8] In contrast, hydrogen production by means of electrocatalytic water splitting is a completely clean method with lower costs and profitable oxygen by-product, which has great potential to produce molecular hydrogen on large scales.[9,10] In electrocatalytic water splitting, platinum based catalysts are used both as cathode and anode due to the high activity of the platinum metal at low overpotentials.[11–13] With its scarcity in the earth's crust (less than 1 $\mu g \cdot kg^{-1}$ availability) and the indispensable applications in catalysis, electronics, jewellery and anti-cancer drugs platinum has inevitably become the most expensive and strategic commodity for the industry nations.[14] Hence, to meet the growing demand and to create higher commercial value, it is of great importance to make every single atom count in electrocatalysis.

Recently, the use of single-atom catalysts on solid supports have emerged as new frontier in electrocatalysis due to the atom-economy, where every single atom is involved in the catalytic process. Single-atom catalysts embedded in rationally designed coordination environments and immobilized on stable supports provide the unique advantage to bridge the gap between homogenous and heterogeneous catalysis and keeping the amount of scarce metals at minimum. The synthetic tools to make such single atoms catalysts using Pt include multi-stage wet-chemical synthesis,[15–18] atomic layer deposition,[12,19,20] electrochemical deposition[21–23] and other elaborative methods.[24]

A more elegant method to provide a well-defined coordination environment for stable single-atom catalysts is the electrochemical grafting method. In attaching diazonium-substituted ligands onto graphitic and metallic surfaces via strong co-valent chemical bond the grafting method has proven as a powerful tool to address interfacial chemistry.[22,25–27]

Herein, we report on a simple single-step-electrochemical grafting technique to make stable Pt single-atom catalysts (PtSAC) embedded in a strong coordination environmental for platinum group metals. The coordination environment is provided by the 2,6:2',2"-terpyridine pincer type ligand[28–30] that allows tailored mass loading by uptake of Pt^{2+} from commercially available platinum salts in aqueous solution. Furthermore, the electro-grafted terpyridine ligand on the 3-dimensional carbon cloth electrode serves as highly efficient metal scavenger for recovering leached platinum from the counter electrode (Fig. 1). Platinum leaching from the counter electrodes during long-term operation in acidic media has been in focus of recent studies questioning the reliability of Pt as counter electrode in membrane-less electrolysers.[31–35] Significant loss of the noble metal stemming from the counter electrode is observed in the electrolyte.[33,36] In this study, leached platinum atoms are scavenged by the terpyridine ligand and utilized *in-situ* as additional single-atom catalysts improving the catalysts performance as the hydrogen evolution reaction progresses.

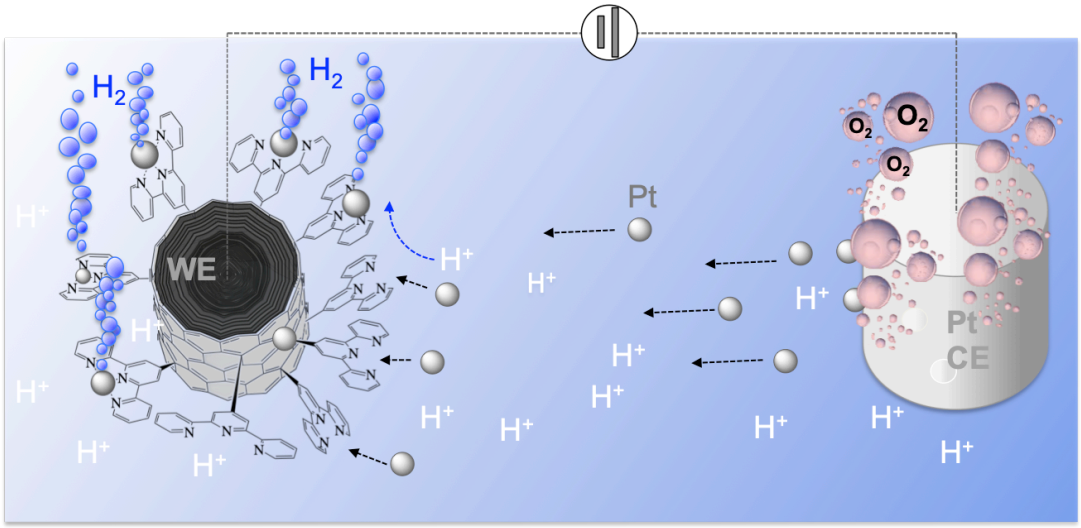

Figure 1: Hydrogen production on Pt single atoms embedded in terpyridine coordination environment electro-grafted onto the carbon cloth (WE) fibre. The electro-grafted ligand acts also as vacancy for leached Pt ions from the counter electrode (CE).

The preparation of the electrocatalyst from commercially available products is non-hazardous, versatile and does not require any elaborative and expensive pre- and/or post-treatment. To the best of our knowledge, this is first report on single-step electro-grafting method to chemically bind 2,6:2',2"-terpyridine directly onto 3D carbon support and fabrication of single-atom catalysts by simple metal uptake from commercially available metal salts.

EXPERIMENTAL

Materials and methods. Sulfuric acid (98%, Scharlau), hydrochloric acid (Sigma Aldrich, analytical grade) and potassium hydroxide (Scharlau, Spain) were diluted with MilliQ water (TOC 1.8 ppm, 18.2 ΩMcm@25°C) to the required molarities in 100 mL volumetric flasks. Sodium nitride, $NaNO_2$, and potassium tetrachloroplatinate, $K_2[PtCl_4]$, were purchased from Sigma Aldrich and used

96 without further purification. 4'-Amino-2,2':6',2'-terpyridine was purchased from Shanghai UCHEM
97 Inc. (Shanghai, China) and used without further purification.
98 Carbon cloth (Plain Carbon Cloth 1071, SKU 591342-1) and 0.03 mg/cm² 20% Platinum on
99 Vulcan – Cloth (W1S1009) were purchased from FuelCellStore (Fuel Cell Etc, USA) and cut into 1 x
100 5 cm^2 pieces to obtain the carbon cloth (CC) and 20% 0.03 mg Pt/C electrodes.
101 X-ray photoelectron spectroscopy (XPS) was performed with a Kratos Ultra DLD spectrometer, using
102 monochromatic Al kα radiation (hν = 1486.7 eV). The system is equipped with a magnetically
103 confined charge compensation system (low energy electrons are confined and transported to the
104 sample surface by magnetic field). Spectra were recorded using an acceleration voltage of 15 keV at a
105 power of 225 W. Survey spectra were collected with a pass energy of 160 eV and an analysis area of
106 300 x 700 μm. Data analysis was performed with CasaXPS software (Casa Software Ltd.) and
107 selected graphs were plotted with the Qti Plot software. XPS spectra of CC electrodes were collected
108 with a SPECS instrument, Berlin (Germany). X-ray emission with the Mg Kα line (12kV-200 W) was
109 used from a no-monochromatic source. High-resolution scans at a pass energy of 10 eV were recorded
110 after a survey scan for characterizing the chemical states. The excitation energy was 1253.6 eV.[37,38]
111 No charging was observed in the obtained spectra thus an usual calibration of C-C to 285.0 eV was
112 not processed. The error bar of the binding energy of peaks fitting is ± 0.15 eV.
113 Raman spectra were acquired using a Witec alpha300R Raman microscope at an excitation
114 laser wavelength of 532 nm with a 40X objective (numerical aperture 0.60). Typical integration times
115 for single Raman spectra were 5 to 15 s and averaged from 2 to 3 repetitions. 10 to 15 spectra were
116 acquired per sample with spectra analysed using Witec project 4.1.
117 Thermogravimetric analysis (TGA) measurements were performed on PerkinElmer TGA
118 8000, with the temperature range of 30 - 1000 °C under nitrogen gas protection, and the heating ramp
119 of 10 °C•min^{-1}. All samples were dried in a vacuum oven at RT prior to the measurements.
120 Electrochemical data were recorded on an AUTOLAB potentiostat (Metrohm, Switzerland) in
121 0.5 M HCl for the electro-grafting step and 0.5 M H_2SO_4 for electrocatalytic studies using modified

carbon cloth as working electrode (WE), a platinum wire or graphite rod as counter electrode (CE) and Ag|AgCl (1M KCl) as reference electrode. Recorded potentials were converted into reversible hydrogen electrode (RHE) as reported elsewhere.[39]

Inductively coupled plasma optical emission spectroscopy (ICP-OES) was conducted on a Perkin Elmer Optima 800 instrument using standard calibration between 10 and 500 ppb Pt^{2+}.

Electro-grafting of the terpyridine ligand onto the plain CC electrode, terpy@CC. In a 20 mL electrochemical cell, 16.8 mg (0.068 mmol) of 4'-amino-2,2':6',2''-terpyridine and 37.4 mg (0.44 mmol) of sodium nitrate were dissolved in 10 mL of 0.5 M HCl solution and purged with N_2 for 15 minutes. Then, 10 consecutive cyclic voltammetry scans were applied at 10 mVs^{-1} between 0.2 and -1.0 volts using the plain carbon cloth (1 x 5 cm) as working, Pt wire as counter and Ag|AgCl (1M KCl) as reference electrode. After the grafting step was finished, the submerged (grafted) surface area of CC was measured and the obtained Terpy@CC electrode was stored in a 0.1 M KOH solution for at least 30 minutes, then washed with MilliQ water, then EtOH and dried in the vacuum oven overnight.

Pt^{2+} uptake by the terpy@CC electrode. The terpy@CC electrodes were cut to small pieces (typically 2 cm x 1 cm) and submerged in dark inside a closed vial containing 20 mL aqueous $K_2[PtCl_4]$ solution with an available concentration of 0.5 ppm Pt^{2+} for 2 h at room temperature (RT). The MilliQ water was purged for at least 30 min with N_2 prior to dissolving the platinum salt. After 2 h uptake, the closed vial was gently shaken and 18 mL of the Pt^{2+} solution was analysed by ICP OES. To validate the Pt^{2+} uptake by terpy@CC, two control experiments were conducted with pure CC electrodes and no absorbent added to the 0.5 ppm Pt^{2+}. In total, four uptake experiments were conducted, and the remaining Pt^{2+} solutions after uptake were analysed by ICP OES. Whereas no concentration difference between both control samples was detected by ICP OES, the concentration difference after uptake by the terpy@CC electrode was calculated to be 0.26 ± 0.02 $\mu g \cdot cm^{-2}$.

RESULTS AND DISCUSSION

Synthesis and performance of the Pt single-atom catalysts in HER

Terpyridine is a versatile ligand in coordination chemistry, it is well-known for its strong binding character to noble metals and has a widespread applications in molecular architectures.[40–45] The plain carbon cloth (CC) has high electrical conductivity and is an ideal support material for self-supported electrocatalysts.[46,47] The flexible 3-dimonsional woven structure that provides relatively large specific surface area can accommodate a high number of grafted ligands via covalent bonds, enabling the combination of single-atom chemistry with 3D supported catalysis. To make the stable 3-dimenisional and metal-chelating electrode, the terpyridine ligand was electro-grafted onto the carbon cloth electrode under cathodic reduction in 0.5 M HCl solution using cyclic voltammetry. 4-Diazonium-2,2':6,2"-terpyridine was generated *in-situ* with sodium nitrite in 0.5 M HCl and subjected to electrochemical grafting (see Experimental and Scheme 1a).[27,48,49] As shown in Fig 2a, a strong reduction event appears at -0.68 V vs. RHE during cathodic cycling in 0.5 M HCl electrolyte solution. The strong reduction event originates from the homolytic cleavage of C-N_2^+ bond creating a terpyridine radical that immediately reacts with the carbon surface (Scheme 1b). Within the subsequent numbers of cathodic sweeps, the intensity of observed reduction peak decreases rapidly, a typical indication for surface saturation with electro-grafted ligands.[50,51] The rapid decrease in the reduction peak and the absence of additional reduction events during progressing cyclic voltammetry sweeps is indicative for single layer grafted terpyridine ligands. Note that, from one single ligand solution a series of terpyridine-grafted CC electrodes could be prepared highlighting the advantage of the electrochemical grafting method. Thermogravimetric analysis shows the ligand being stable on the carbon cloth surface up to 300^{o}C (terpy@CC, Fig. 2b) and XPS surface analysis of the electro-grafted carbon cloth electrode detected high content (up to 10%) of nitrogen on the surface, which is attributed to the ligand (vide infra).

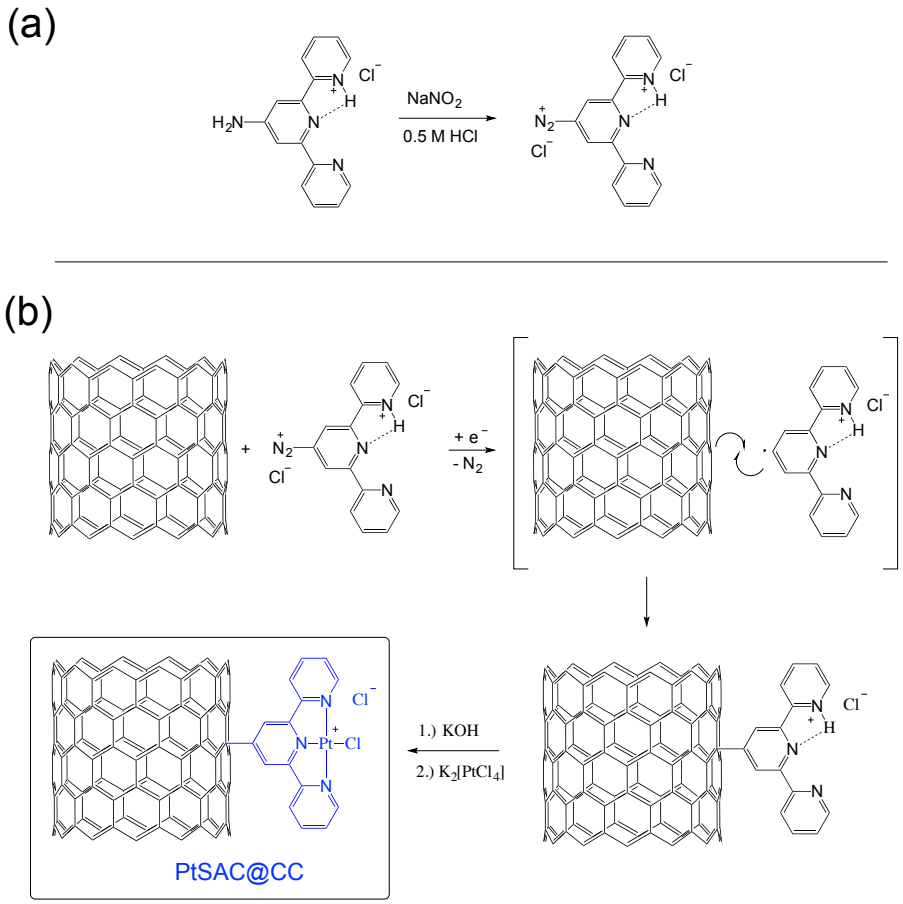

Scheme 1: **(a)** *In-situ* preparation of 4-diazonium 2,2':6,2"-terpyridine in 0.5 M HCl electrolyte solution using sodium nitrite as oxidant and, **(b)** subsequent electrochemical grafting of the terpyridine ligand onto the 3-dimenisonal carbon cloth at -0.68 V vs. RHE. The synthesis of the platinum single-atom electrocatalyst, PtSAC, is achieved by metal uptake from aqueous $K_2[PtCl_4]$ solution.

To make the single-atom Pt electrocatalyst (PtSAC@CC-0.5), the terpy-grafted CC electrode, terpy@CC, was submerged in aqueous potassium tetrachloroplatinate solution (0.5 ppm Pt^{2+}) for 2 h at RT. In our studies, we found that increased temperature, exposure to light and presence of dissolved oxygen caused formation of Pt deposition on the non-grafted CC electrode itself. Hence, to avoid deposition of nano-particulate platinum on the CC surface, the Pt^{+2} uptake was conducted under N_2 protection and in the dark. Under these conditions, repeated uptake experiments from 0.5 ppm Pt^{2+} ions revealed mass loadings of 0.26 ± 0.02 μg•cm^{-2} of platinum on the terpy@CC electrodes, whereas no Pt uptake from pure CC could be detected by ICP OES.

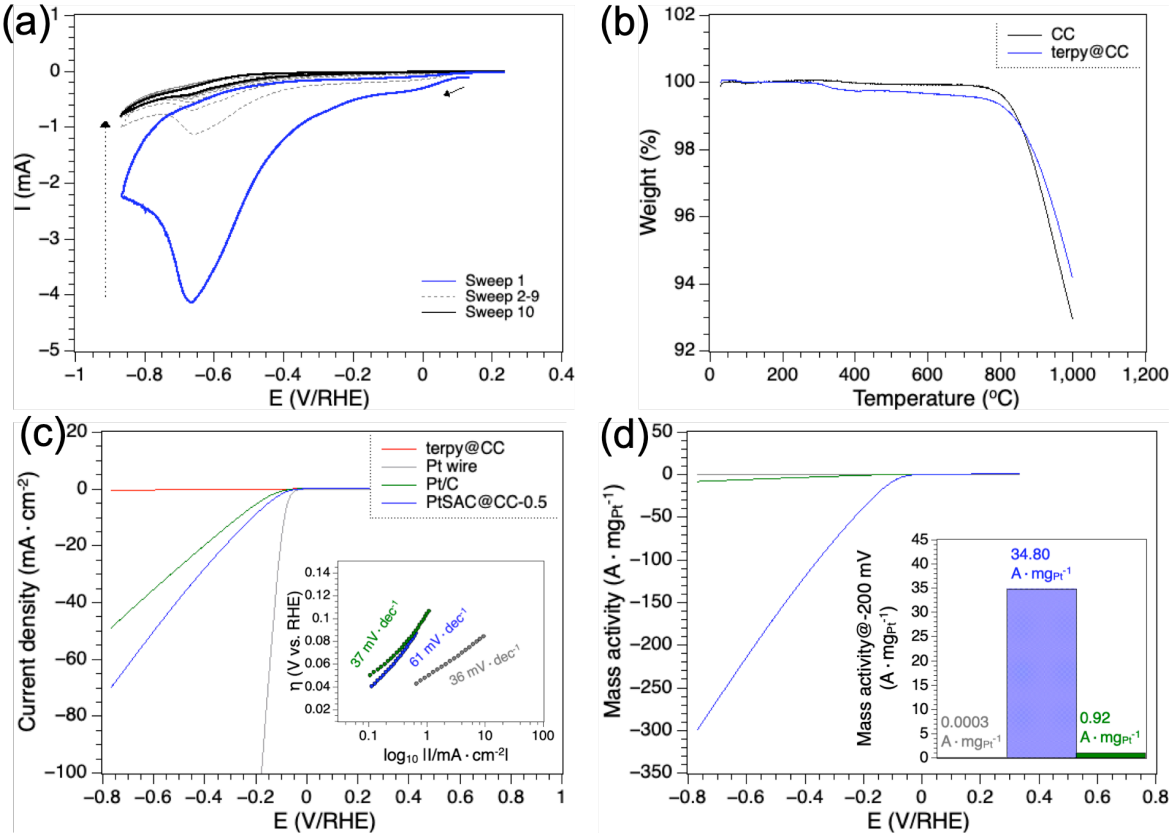

Figure 2: Recorded cyclic voltammogram of electro-grafting 4-amino terpyridine onto the carbon electrode in 0.5 M HCl electrolyte solution. (b) TGA thermogram of the electro-grafted ligand (terpy@CC) compared to the blank support carbon cloth (CC). (c) Linear sweep voltammogram of the Pt single-atom catalyst (PtSAC@CC-0.5) compared to the free ligand terpy@CC (red), commercial catalyst 0.03 mg 20% Pt/C@CC (green) and the Pt wire (grey); inset shows the calculated Tafel slopes with their respective colour scheme. (d) Calculated mass activity of the catalysts as function of applied potential vs. RHE in their respective colour; inset shows comparative mass activity at the overpotential of 200 mV.

The HER activity of the single-atom Pt catalyst, PtSAC@CC-0.5, was studied in 0.5 M H_2SO_4 solution using a Pt wire and Ag|AgCl (1 M KCl) as counter and reference electrode, respectively. For comparisons, commercially available benchmark catalyst on carbon cloth, 20% 0.03 mg Pt/C, a platinum wire and the free ligand electro-grafted onto the CC electrode were tested under the same conditions. For a better accuracy of the performance data and to avoid potential metal

leaching from the Pt counter electrode and re-deposition onto the working electrode in acidic media, only 10 cyclic voltammetry sweeps at 10 $mV \cdot s^{-1}$ were applied. Figure 2c shows the last forward sweep of the recorded cyclic voltammograms, each. It appears that the single atom catalyst slightly outperforms the commercially available benchmark catalyst, 20% 0.03 mg Pt/C, when normalised to the geometric surface area. To generate 10 $mA \cdot cm^{-2}$, PtSAC@CC-0.5 requires 210 mV vs. RHE, which is 59 mV lower than Pt/C. The Tafel slopes were calculated in the low overpotential range of 40-110 mV to be 61, 37 and 36 $mV \cdot dec^{-1}$ for the PtSAC@CC-0.5, Pt/C and the Pt wire, respectively.

Table 1: Calculated mass activity ratios of the PtSAC and 20% Pt/C studied in this work and compared to the activity ratios of Pt single-atom catalysts reported in literature.

Overpotential	Mass activity ratio between studied catalyst and 20% Pt/C	
η (V/RHE)	This work	Literature
50 mV	77.1	74.4[52], 40[53], 37.4[12], 4.3[13]
100 mV	51.3	47.56[53], 26.9[54], 6.1[13]
200 mV	37.8	6.3[55]

To compare the activity with reported platinum single-atom catalysts the linear sweep voltammograms in Fig. 2c were converted into the mass activities (Fig. 2d). Here, our PtSAC@CC-0.5 outperforms by far the Pt wire and the commercial catalysts Pt/C making literally every single atom count in the hydrogen evolution reaction. When normalised to the mass loading of Pt/C, the ultra-low loading of 0.26 ± 0.02 $\mu g \cdot cm^{-2}$ platinum places the single-atom catalyst, PtSAC@CC-0.5 in an highly competitive position. As summarized in Table 1, the PtSAC@CC-0.5 self-supported on the 3D carbon cloth electrode is slightly better than the highest reported mass activities at overpotentials of 50, 100 and 200 mV, respectively.

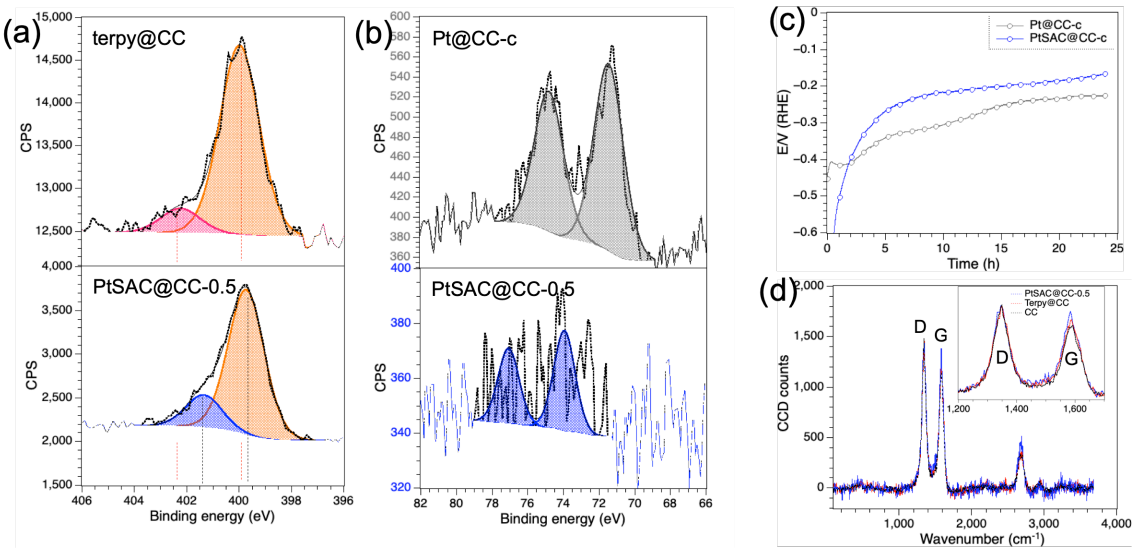

Figure 3: (a) Fitted N1s and (b) Pt4f core level spectra of the electro-grafted terpyridine onto carbon cloth (terpy@CC), ultra-low platinum-loaded single atom catalyst (PtSAC@CC-0.5) and Pt-loaded carbon cloth after 24 h chronoamperometric (Pt@CC-c); the ultra-low loading of the electro-grafted terpy@CC electrode was carried out from 0.5 ppm Pt^{2+} ion solution and the Pt-loading onto CC electrode stems from Pt leaching from the CE and re-deposition onto the WE; (c) Chronoamperometric HER at 10 $mA{\cdot}cm^{-2}$ for 24 h on PtSAC@CC-0.5 and CC electrode. Due to the Pt leaching and re-deposition onto the working electrodes, both electrodes became PtSAC@CC-c and Pt@CC-c; (d) Overlapped D and G Raman bands of CC, Pt@CC, terpy@CC and PtSAC@CC-0.5.

Thorough surface analysis by X-ray photoelectron spectroscopy (XPS) was carried out to investigate the valence state of the metal in PtSAC@CC-0.5 and to understand the participation of the coordination environment in the electro-grafted terpyridine ligand. The fitted N(1s) and Pt(4f) core level spectra are shown in Fig. 3 and summarized in Table 2. Electro-grafted CC showed under XPS more than 10% nitrogen with the N1s core level spectrum fitted to a main peak at 400 eV accompanied by a peak at 402.3 eV (Fig. 3a), which is assigned to residual $=N\text{-}H^{+}$ after electro-grafting the ligand under acidic conditions (see mechanism in Scheme 1). After Pt uptake from 0.5 ppm Pt^{2+} ions, both N peaks were shifted toward lower binding energies (BE) where the $=N\text{-}H^{+}$ peak featuring a significant drop (ΔBE 1.0 eV). The XPS core level spectra of platinum exhibit two

asymmetric components in the Pt4f region ($Pt4f_{7/2}$ and $Pt4f_{5/2}$ spin orbital splitting) with a typical peak separation of 3.33 eV. Leached platinum that only originates from the counter electrode during 24 hours chronoamperometric water splitting and re-deposited onto the WE (Pt@CC-c, Fig. 3b, top panel) exhibits only zero-valent platinum (Pt^0), whereas the terpyridine-grafted electrode pre-loaded with Pt^{2+} ions from 0.5 ppm solution shows trace amounts Pt^{2+} at 73.8 eV as oxide under XPS (see Fig. 3b bottom panel and Table 2).[53,56] It has to be noticed that due to the ultra-low Pt loading, the Pt peak is ambiguous thus the fitting could yield a larger error bar but the binding energy of peaks can still be assigned to Pt^{2+}. Although 10 linear sweeps were applied to PtSAC@CC-0.5, XPS analysis of the electrode showed no indication of reduced platinum.

Table 2: Fitted XPS core level data in Pt4f, their atomic composition and ratios as well as the Raman D/G ratios of studied electrodes.

Electrode	% C	% O	% N	% Pt	N/Pt	Pt^0	Pt^{2+}	D/G
CC	95.06	4.94	0	0	-	-	-	1.28
Pt@CC-c	96.15	3.67		0.19	-	74.9 71.5	- -	1.14
Terpy@CC	78.41	11.17	10.71	-	-	-	-	1.17
PtSAC@CC-0.5	76.05	11.62	12.27	0.03	409	- -	77.1 73.9	1.07
PtSAC@CC-0.5c	72.83	14.38	11.09	1.46	7.6	74.8 71.4	77.3 73.9	
PtSAC@CC-165	66.85	18.85	9.50	2.81	3.38	75.4 72.0	77.0 73.7	

After chronoamperometric water splitting at PtSAC-0.5 (Fig. 3c), XPS detected a mixture of zero- and bi-valent platinum on the electrode, where Pt^0 is major valence state (PtSAC@CC-0.5c in Fig. 4b). In stark contrast to the ligand-free CC electrode, much stronger deposition onto the terpy-grafted WE was detected by XPS. The Pt content increased from 0.03% to 1.46% after 24 h operation, whereas the increase of Pt content on ligand-free CC was only by 0.19%. This observation is also indicated by the steep decrease of the overpotential at the PtSAC-0.5c electrode during the

chronoamperometric water splitting (see Fig. 3c) suggesting that leached Pt from the counter electrode is immediately bound into chelating interface of the working electrode.

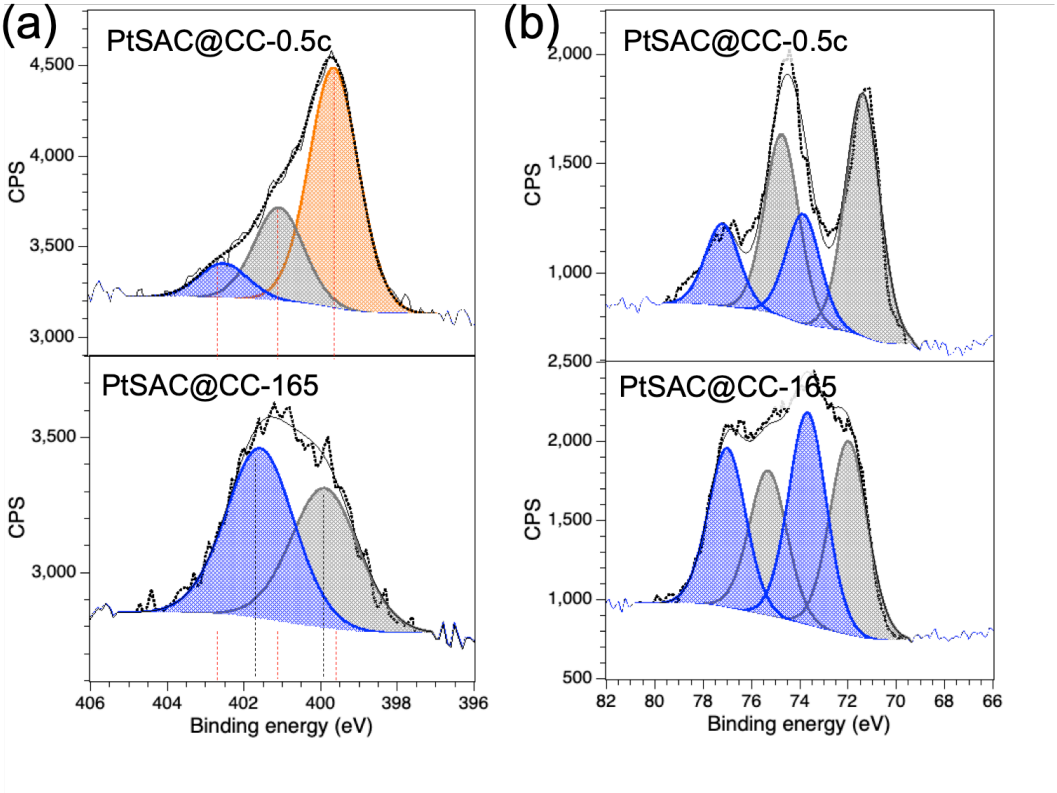

Figure 4: Fitted (a) N1s and (b) Pt4f core level spectra of the ultra-low platinum-loaded single atom catalyst (PtSAC@CC-0.5c) after 24 h chronoamperometry (top panels) and after uptake of Pt^{2+} from 165 ppm Pt ion solution (bottom panels).

When using graphite rod as counter electrode in a separate chronoamperometric HER experiment on PtSAC-0.5, XPS detected Pt^{2+} as only valence state with no loss of metal after 3 h of operation suggesting that presence of the Pt^0 in the previous experiment (PtSAC-0.5c) was largely contributed by leached metal from the Pt CE (Fig. S1, Supporting Information). Using again Pt as CE in further control experiments with 8 hours chronoamperometric HER on the PtSAC@CC-0.5 and CC electrodes showed 240-260 ppb Pt being leached into the electrolyte solution, when the electrolytes were analysed by ICP OES. It was also found that re-deposited Pt onto CC in both valence states Pt^0

and Pt^{2+} was removed by more than 71% when the working electrode was sonicated for 40 minutes in pure H_2O and then subjected to surface analysis by XPS (see Fig. 5b). In contrast, bound Pt^{2+} into the terpy@CC electrode was not removed from the chelating pockets after the same time of sonication (Fig. 5a). Again, this method clearly highlights the main advantage of the terpyridine ligand on CC support as it acts as efficient scavenger for leached platinum.

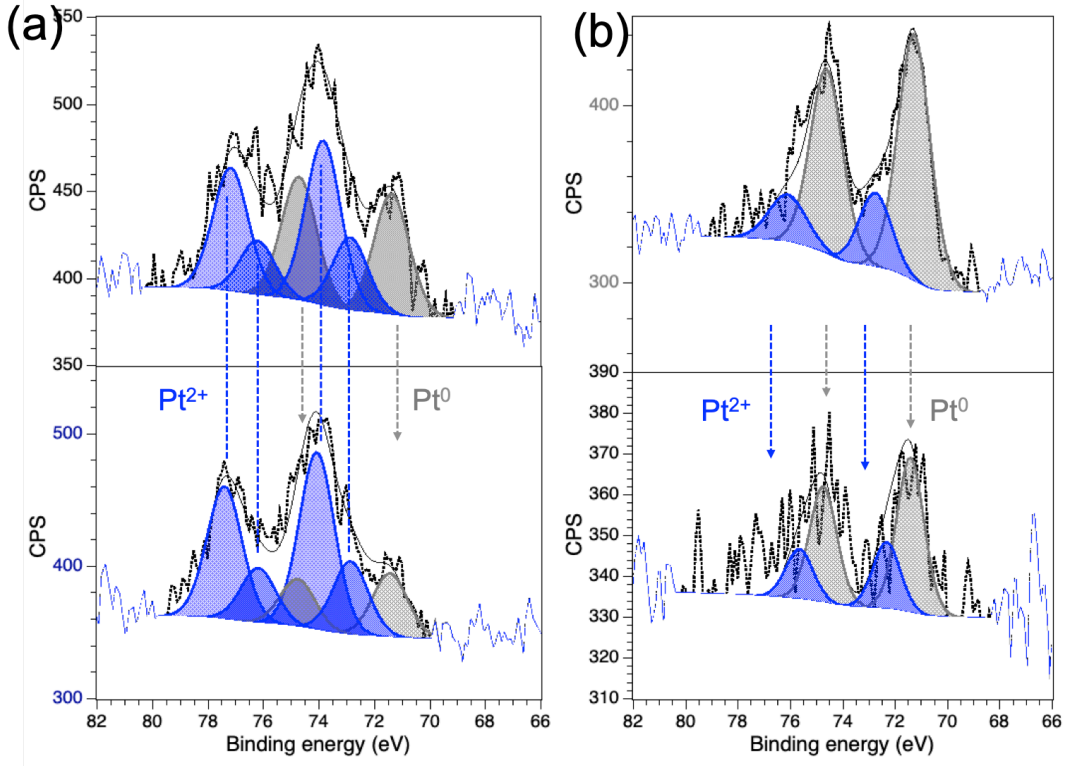

Figure 5: (a) Fitted Pt4f core level spectra of the ultra-low platinum-loaded single atom catalyst (PtSAC@CC-0.5) after 8 h chronoamperometry (top panels) and after 40 min sonication (bottom panel) using the Pt wire as CE; (b) Fitted Pt4f core level spectra of leached Pt and deposited onto CC after 8 h chronoamperometry (top panels) and after 40 min sonication (bottom panel) using the Pt wire as CE.

As shown in Fig. 4a (top panel), three components were fitted to the N1s core level spectrum of PtSAC@CC-0.5c, that is assigned to the nitrogen in the free ligand (orange) and the N-donors bound to Pt^0 (grey) and Pt^{2+} (blue), respectively. Although significant amounts of Pt were leached and

bound to the terpy@CC interface, only less than a half of the available ligands were occupied by Pt (N/Pt ratio of 7.6 in Table 2). A nearly full saturation with Pt was found in uptake experiments within 2 hours, when the concentration of the available Pt ions was increased to 165 ppm (N/Pt ratio of 3.38 in PtSAC@CC-165, Table 2). Notably, the fitted components in Pt4f core level data revealed high amounts of zero-valent platinum in PtSAC@CC-165, although the uptake was from Pt^{2+} ions. In line with the reported studies in the literature, it appears to be difficult to obtain either one of the valence Pt^0, Pt^{2+} or Pt^{4+} at higher metal loadings.[57] Of particular note is also the observed I_D/I_G ratio in the Raman spectra (Fig. 3d). The intensity and positions of Raman peaks can provide important structural information for the carbon samples. The G peak between 1560 to 1600 cm^{-1} is associated with a vibrational mode of sp^2-hybridized graphene planes. The D peak at 1300 to 1400 cm^{-1} is the band associated with defects. The ratio of D band to G band peak intensities, I_D/I_G, has been used to probe the level of disorder of carbon materials.[52] Non-grafted CC displays the highest ratio between the D- and G-band indicative for highest defects of the carbon surface in this series. As the surface is manipulated further, more symmetry is induced as indicated in the decay of the I_D/I_G ratio that approaches a ratio of 1/1. This tendency has also been observed in similar catalysts systems and explained by coverage of the defects after manipulating the carbon fibre surface (Table 2).[52]

CONCLUSIONS

Functionalisation of the 3D carbon cloth surface with well-defined coordination environment by simple electrochemical grafting methods enables to access ultra-low loaded and high performing single atom catalysts for electrocatalytic applications. In this study, using the terpyridine ligand as strong chelator for noble metals, platinum single-atom catalysts were made in two simple steps without involving elaborative synthetic methods. The obtained PtSAC@CC-0.5 revealed the lowest reported mass loading of 0.26 ± 0.02 $\mu g \cdot cm^{-2}$ and the highest reported mass activity ratio of 77.1

$A \bullet g_{Pt}^{-1}$ at η = 50 mV/RHE in the electrocatalytic hydrogen production compared to the benchmark catalyst Pt/C. This method provides dual benefit for the scarcity of the noble metals. In pushing the Pt value down to 0.1 US$•$m^{-2}$ compared to 2.30 US$•$m^{-2}$ for 20% 0.03 mg Pt/C (see Supporting Information) it makes literally every single atom count in electrocatalysis and recovers leached metal from counter electrodes at the same time.

ACKNOWLEDGEMENT

S. E. and M. R. A. thank the Australian Government through the Australian Research Council's Discovery Projects funding scheme (project DP210101243). The authors acknowledge the expertise, equipment and support provided by Microscopy Australia and the Australian National Fabrication Facility (ANFF) at the South Australian nodes under the National Collaborative Research Infrastructure Strategy. The authors acknowledge the expertise, equipment and support provided by Flinders Microscopy and Microanalysis (FMMA) at Flinders University. This project was also supported by the French-Australian Research Network on Energy and Conversion through the International Research Network (project IRN FACES).

AUTHORS CONTRIBUTION

P.-W. Y. and S. E. contributed equally.

CONFLICT OF INTEREST

The authors declare no conflict of interest.

ABBREVIATIONS

CC – Carbon cloth electrode.

terpy – Terpyridine ligand

terpy@CC – terpyridine ligand electro-grafted onto the CC surface

PtSAC – Platinum single-atom catalyst.

PtSAC@CC – Platinum single-atom catalyst bound into terpy@CC.

PtSAC@CC-0.5 – PtSAC@CC obtained from 0.5 ppm Pt^{2+} solution.

PtSAC@CC-0.5c – PtSAC@CC obtained from 0.5 ppm Pt^{2+} solution and after chronoamperometric HER.

PtSAC@CC-165 – PtSAC@CC obtained from 165 ppm Pt^{2+} solution.

Pt@CC-c – leached platinum from Pt CE and re-deposited onto the CC working electrode after chronoamperometric HER.

REFERENCES

(1) Abe, J. O.; Popoola, A. P. I.; Ajenifuja, E.; Popoola, O. M. Hydrogen Energy, Economy and Storage: Review and Recommendation. *International Journal of Hydrogen Energy* **2019**, *44* (29), 15072–15086. https://doi.org/10.1016/j.ijhydene.2019.04.068.

(2) Pudukudy, M.; Yaakob, Z.; Mohammad, M.; Narayanan, B.; Sopian, K. Renewable Hydrogen Economy in Asia – Opportunities and Challenges: An Overview. *Renewable and Sustainable Energy Reviews* **2014**, *30*, 743–757. https://doi.org/10.1016/j.rser.2013.11.015.

(3) Hsu, S.-H.; Miao, J.; Zhang, L.; Gao, J.; Wang, H.; Tao, H.; Hung, S.-F.; Vasileff, A.; Qiao, S. Z.; Liu, B. An Earth-Abundant Catalyst-Based Seawater Photoelectrolysis System with 17.9% Solar-to-Hydrogen Efficiency. *Adv. Mater.* **2018**, *30* (18), 1707261. https://doi.org/10.1002/adma.201707261.

(4) Lin, L.; Zhou, W.; Gao, R.; Yao, S.; Zhang, X.; Xu, W.; Zheng, S.; Jiang, Z.; Yu, Q.; Li, Y.-W.; Shi, C.; Wen, X.-D.; Ma, D. Low-Temperature Hydrogen Production from Water and Methanol Using Pt/α-MoC Catalysts. *Nature* **2017**, *544* (7648), 80–83. https://doi.org/10.1038/nature21672.

(5) Momirlan, M.; Veziroglu, T. N. Current Status of Hydrogen Energy. *Renewable and Sustainable Energy Reviews* **2002**, *6* (1–2), 141–179. https://doi.org/10.1016/S1364-0321(02)00004-7.
(6) LeValley, T. L.; Richard, A. R.; Fan, M. The Progress in Water Gas Shift and Steam Reforming Hydrogen Production Technologies – A Review. *International Journal of Hydrogen Energy* **2014**, *39* (30), 16983–17000. https://doi.org/10.1016/j.ijhydene.2014.08.041.
(7) Palo, D. R.; Dagle, R. A.; Holladay, J. D. Methanol Steam Reforming for Hydrogen Production. *Chem. Rev.* **2007**, *107* (10), 3992–4021. https://doi.org/10.1021/cr050198b.
(8) Holladay, J. D.; Hu, J.; King, D. L.; Wang, Y. An Overview of Hydrogen Production Technologies. *Catalysis Today* **2009**, *139* (4), 244–260. https://doi.org/10.1016/j.cattod.2008.08.039.
(9) Nong, H. N.; Gan, L.; Willinger, E.; Teschner, D.; Strasser, P. IrOx Core-Shell Nanocatalysts for Cost- and Energy-Efficient Electrochemical Water Splitting. *Chem. Sci.* **2014**, *5* (8), 2955–2963. https://doi.org/10.1039/C4SC01065E.
(10) You, B.; Sun, Y. Innovative Strategies for Electrocatalytic Water Splitting. *Acc. Chem. Res.* **2018**, *51* (7), 1571–1580. https://doi.org/10.1021/acs.accounts.8b00002.
(11) Reier, T.; Oezaslan, M.; Strasser, P. Electrocatalytic Oxygen Evolution Reaction (OER) on Ru, Ir, and Pt Catalysts: A Comparative Study of Nanoparticles and Bulk Materials. *ACS Catal.* **2012**, *2* (8), 1765–1772. https://doi.org/10.1021/cs3003098.
(12) Cheng, N.; Stambula, S.; Wang, D.; Banis, M. N.; Liu, J.; Riese, A.; Xiao, B.; Li, R.; Sham, T.-K.; Liu, L.-M.; Botton, G. A.; Sun, X. Platinum Single-Atom and Cluster Catalysis of the Hydrogen Evolution Reaction. *Nat Commun* **2016**, *7* (1), 13638. https://doi.org/10.1038/ncomms13638.
(13) Cheng, X.; Li, Y.; Zheng, L.; Yan, Y.; Zhang, Y.; Chen, G.; Sun, S.; Zhang, J. Highly Active, Stable Oxidized Platinum Clusters as Electrocatalysts for the Hydrogen Evolution Reaction. *Energy Environ. Sci.* **2017**, *10* (11), 2450–2458. https://doi.org/10.1039/C7EE02537H.
(14) Reith, F.; Campbell, S. G.; Ball, A. S.; Pring, A.; Southam, G. Platinum in Earth Surface Environments. *Earth-Science Reviews* **2014**, *131*, 1–21. https://doi.org/10.1016/j.earscirev.2014.01.003.
(15) Liang, S.; Hao, C.; Shi, Y. The Power of Single-Atom Catalysis. *ChemCatChem* **2015**, *7* (17), 2559–2567. https://doi.org/10.1002/cctc.201500363.
(16) Elmas, S.; Beelders, W.; Bradley, S. J.; Kroon, R.; Laufersky, G.; Andersson, M.; Nann, T. Platinum Terpyridine Metallopolymer Electrode as Cost-Effective

Replacement for Bulk Platinum Catalysts in Oxygen Reduction Reaction and Hydrogen Evolution Reaction. *ACS Sustainable Chemistry & Engineering* **2017**, *5* (11), 10206–10214. https://doi.org/10.1021/acssuschemeng.7b02198.

(17) Pu, Z.; Amiinu, I. S.; Cheng, R.; Wang, P.; Zhang, C.; Mu, S.; Zhao, W.; Su, F.; Zhang, G.; Liao, S.; Sun, S. Single-Atom Catalysts for Electrochemical Hydrogen Evolution Reaction: Recent Advances and Future Perspectives. *Nano-Micro Lett.* **2020**, *12* (1), 21. https://doi.org/10.1007/s40820-019-0349-y.

(18) Cheng, N.; Zhang, L.; Doyle-Davis, K.; Sun, X. Single-Atom Catalysts: From Design to Application. *Electrochem. Energ. Rev.* **2019**, *2* (4), 539–573. https://doi.org/10.1007/s41918-019-00050-6.

(19) Piernavieja-Hermida, M.; Lu, Z.; White, A.; Low, K.-B.; Wu, T.; Elam, J. W.; Wu, Z.; Lei, Y. Towards ALD Thin Film Stabilized Single-Atom Pd $_1$ Catalysts. *Nanoscale* **2016**, *8* (33), 15348–15356. https://doi.org/10.1039/C6NR04403D.

(20) Sun, S.; Zhang, G.; Gauquelin, N.; Chen, N.; Zhou, J.; Yang, S.; Chen, W.; Meng, X.; Geng, D.; Banis, M. N.; Li, R.; Ye, S.; Knights, S.; Botton, G. A.; Sham, T.-K.; Sun, X. Single-Atom Catalysis Using Pt/Graphene Achieved through Atomic Layer Deposition. *Sci Rep* **2013**, *3* (1), 1775. https://doi.org/10.1038/srep01775.

(21) Zhang, L.; Han, L.; Liu, H.; Liu, X.; Luo, J. Potential-Cycling Synthesis of Single Platinum Atoms for Efficient Hydrogen Evolution in Neutral Media. *Angew. Chem. Int. Ed.* **2017**, *56* (44), 13694–13698. https://doi.org/10.1002/anie.201706921.

(22) Tavakkoli, M.; Holmberg, N.; Kronberg, R.; Jiang, H.; Sainio, J.; Kauppinen, E. I.; Kallio, T.; Laasonen, K. Electrochemical Activation of Single-Walled Carbon Nanotubes with Pseudo-Atomic-Scale Platinum for the Hydrogen Evolution Reaction. *ACS Catal.* **2017**, *7* (5), 3121–3130. https://doi.org/10.1021/acscatal.7b00199.

(23) Zhang, J.; Zhao, Y.; Guo, X.; Chen, C.; Dong, C.-L.; Liu, R.-S.; Han, C.-P.; Li, Y.; Gogotsi, Y.; Wang, G. Single Platinum Atoms Immobilized on an MXene as an Efficient Catalyst for the Hydrogen Evolution Reaction. *Nat Catal* **2018**, *1* (12), 985–992. https://doi.org/10.1038/s41929-018-0195-1.

(24) Chen, Y.; Ji, S.; Chen, C.; Peng, Q.; Wang, D.; Li, Y. Single-Atom Catalysts: Synthetic Strategies and Electrochemical Applications. *Joule* **2018**, *2* (7), 1242–1264. https://doi.org/10.1016/j.joule.2018.06.019.

(25) Gautier, C.; López, I.; Breton, T. A Post-Functionalization Toolbox for Diazonium (Electro)-Grafted Surfaces: Review of the Coupling Methods. *Mater. Adv.* **2021**, *2* (9), 2773–2810. https://doi.org/10.1039/D1MA00077B.

(26) Bangle, R.; Sampaio, R. N.; Troian-Gautier, L.; Meyer, G. J. Surface Grafting of Ru(II) Diazonium-Based Sensitizers on Metal Oxides Enhances Alkaline Stability for

Solar Energy Conversion. *ACS Appl. Mater. Interfaces* **2018**, *10* (3), 3121–3132. https://doi.org/10.1021/acsami.7b16641.

(27) Ghasemi, E.; Alimardani, E.; Shams, E.; Koohmareh, G. A. Modification of Glassy Carbon Electrode with Iron-Terpyridine Complex and Iron-Terpyridine Complex Covalently Bonded to Ordered Mesoporous Carbon Substrate: Preparation, Electrochemistry and Application to H 2 O 2 Determination. *Journal of Electroanalytical Chemistry* **2017**, *789*, 92–99. https://doi.org/10.1016/j.jelechem.2017.01.043.

(28) Albrecht, M.; van Koten, G. Platinum Group Organometallics Based on "Pincer" Complexes: Sensors, Switches, and Catalysts. *Angewandte Chemie International Edition* **2001**, *40* (20), 3750–3781. https://doi.org/10.1002/1521-3773(20011015)40:20<3750::AID-ANIE3750>3.0.CO;2-6.

(29) Klein, A.; Elmas, S.; Butsch, K. Oxido Pincer Ligands - Exploring the Coordination Chemistry of Bis(Hydroxymethyl)Pyridine Ligands for the Late Transition Metals. *European Journal of Inorganic Chemistry* **2009**, *2009* (15), 2271–2281. https://doi.org/10.1002/ejic.200900023.

(30) Klein, A.; Butsch, K.; Elmas, S.; Biewer, C.; Heift, D.; Nitsche, S.; Schlipf, I.; Bertagnolli, H. Oxido-Pincer Complexes of Copper(II) – An EXAFS and EPR Study of Mono- and Binuclear [(PydotH2)CuCl2]n (N=1 or 2). *Polyhedron* **2012**, *31* (1), 649–656. https://doi.org/10.1016/j.poly.2011.10.023.

(31) Chen, R.; Yang, C.; Cai, W.; Wang, H.-Y.; Miao, J.; Zhang, L.; Chen, S.; Liu, B. Use of Platinum as the Counter Electrode to Study the Activity of Nonprecious Metal Catalysts for the Hydrogen Evolution Reaction. *ACS Energy Lett.* **2017**, *2* (5), 1070–1075. https://doi.org/10.1021/acsenergylett.7b00219.

(32) Lee, J.; Bang, J. H. Reliable Counter Electrodes for the Hydrogen Evolution Reaction in Acidic Media. *ACS Energy Lett.* **2020**, *5* (8), 2706–2710. https://doi.org/10.1021/acsenergylett.0c01537.

(33) Gu, C.; Norris, B. C.; Fan, F.-R. F.; Bielawski, C. W.; Bard, A. J. Is Base-Inhibited Vapor Phase Polymerized PEDOT an Electrocatalyst for the Hydrogen Evolution Reaction? Exploring Substrate Effects, Including Pt Contaminated Au. *ACS Catalysis* **2012**, *2* (5), 746–750. https://doi.org/10.1021/cs3000107.

(34) Tian, M.; Cousins, C.; Beauchemin, D.; Furuya, Y.; Ohma, A.; Jerkiewicz, G. Influence of the Working and Counter Electrode Surface Area Ratios on the Dissolution of Platinum under Electrochemical Conditions. *ACS Catal.* **2016**, *6* (8), 5108–5116. https://doi.org/10.1021/acscatal.6b00200.

(35) Esposito, D. V. Membraneless Electrolyzers for Low-Cost Hydrogen Production in a Renewable Energy Future. *Joule* **2017**, *1* (4), 651–658. https://doi.org/10.1016/j.joule.2017.07.003.

(36) Winther-Jensen, B.; Fraser, K.; Ong, C.; Forsyth, M.; MacFarlane, D. R. Conducting Polymer Composite Materials for Hydrogen Generation. *Advanced Materials* **2010**, *22* (15), 1727–1730. https://doi.org/10.1002/adma.200902934.
(37) Ilton, E. S.; Post, J. E.; Heaney, P. J.; Ling, F. T.; Kerisit, S. N. XPS Determination of Mn Oxidation States in Mn (Hydr)Oxides. *Applied Surface Science* **2016**, *366*, 475–485. https://doi.org/10.1016/j.apsusc.2015.12.159.
(38) Shircliff, R. A.; Stradins, P.; Moutinho, H.; Fennell, J.; Ghirardi, M. L.; Cowley, S. W.; Branz, H. M.; Martin, I. T. Angle-Resolved XPS Analysis and Characterization of Monolayer and Multilayer Silane Films for DNA Coupling to Silica. *Langmuir* **2013**, *29* (12), 4057–4067. https://doi.org/10.1021/la304719y.
(39) Elmas, S.; Macdonald, T.; Skinner, W.; Andersson, M.; Nann, T. Copper Metallopolymer Catalyst for the Electrocatalytic Hydrogen Evolution Reaction (HER). *Polymers* **2019**, *11* (1), 110. https://doi.org/10.3390/polym11010110.
(40) Cummings, S. D. Platinum Complexes of Terpyridine: Synthesis, Structure and Reactivity. *Coordination Chemistry Reviews* **2009**, *253* (3–4), 449–478. https://doi.org/10.1016/j.ccr.2008.04.013.
(41) Swiegers, G. F.; Malefetse, T. J. New Self-Assembled Structural Motifs in Coordination Chemistry. *Chem. Rev.* **2000**, *100* (9), 3483–3538. https://doi.org/10.1021/cr990110s.
(42) Hofmeier, H.; Schubert, U. S. Recent Developments in the Supramolecular Chemistry of Terpyridine–Metal Complexes. *Chem. Soc. Rev.* **2004**, *33* (6), 373–399. https://doi.org/10.1039/B400653B.
(43) Whittell, G. R.; Hager, M. D.; Schubert, U. S.; Manners, I. Functional Soft Materials from Metallopolymers and Metallosupramolecular Polymers. *Nature Materials* **2011**, *10* (3), 176–188. https://doi.org/10.1038/nmat2966.
(44) Dewi, M. R.; Gschneidtner, T. A.; Elmas, S.; Ranford, M.; Moth-Poulsen, K.; Nann, T. Monofunctionalization and Dimerization of Nanoparticles Using Coordination Chemistry. *ACS Nano* **2015**, *9* (2), 1434–1439. https://doi.org/10.1021/nn5058408.
(45) Gao, Z.; Han, Y.; Gao, Z.; Wang, F. Multicomponent Assembled Systems Based on Platinum(II) Terpyridine Complexes. *Acc. Chem. Res.* **2018**, *51* (11), 2719–2729. https://doi.org/10.1021/acs.accounts.8b00340.
(46) Tian, J.; Liu, Q.; Asiri, A. M.; Sun, X. Self-Supported Nanoporous Cobalt Phosphide Nanowire Arrays: An Efficient 3D Hydrogen-Evolving Cathode over the Wide Range of PH 0–14. *J. Am. Chem. Soc.* **2014**, *136* (21), 7587–7590. https://doi.org/10.1021/ja503372r.

(47) Sun, H.; Yan, Z.; Liu, F.; Xu, W.; Cheng, F.; Chen, J. Self-Supported Transition-Metal-Based Electrocatalysts for Hydrogen and Oxygen Evolution. *Adv. Mater.* **2020**, *32* (3), 1806326. https://doi.org/10.1002/adma.201806326.

(48) Tregubov, A. A.; Vuong, K. Q.; Luais, E.; Gooding, J. J.; Messerle, B. A. Rh(I) Complexes Bearing *N* , *N* and *N* , *P* Ligands Anchored on Glassy Carbon Electrodes: Toward Recyclable Hydroamination Catalysts. *J. Am. Chem. Soc.* **2013**, *135* (44), 16429–16437. https://doi.org/10.1021/ja405783g.

(49) Binding, S. C.; Pernik, I.; Gonçales, V. R.; Wong, C. M.; Webster, R. F.; Cheong, S.; Tilley, R. D.; Garcia-Bennett, A. E.; Gooding, J. J.; Messerle, B. A. Simultaneous Functionalization of Carbon Surfaces with Rhodium and Iridium Organometallic Complexes: Hybrid Bimetallic Catalysts for Hydroamination. *Organometallics* **2019**, *38* (4), 780–787. https://doi.org/10.1021/acs.organomet.8b00726.

(50) Pinson, J.; Podvorica, F. Attachment of Organic Layers to Conductive or Semiconductive Surfaces by Reduction of Diazonium Salts. *Chem. Soc. Rev.* **2005**, *34* (5), 429. https://doi.org/10.1039/b406228k.

(51) Elmas, S.; Skipper, K.; Salehifar, N.; Jamieson, T.; Andersson, G. G.; Nydén, M.; Leterme, S. C.; Andersson, M. R. Cyclic Copper Uptake and Release from Natural Seawater—A Fully Sustainable Antifouling Technique to Prevent Marine Growth. *Environ. Sci. Technol.* **2021**, *55* (1), 757–766. https://doi.org/10.1021/acs.est.0c06231.

(52) Ji, J.; Zhang, Y.; Tang, L.; Liu, C.; Gao, X.; Sun, M.; Zheng, J.; Ling, M.; Liang, C.; Lin, Z. Platinum Single-Atom and Cluster Anchored on Functionalized MWCNTs with Ultrahigh Mass Efficiency for Electrocatalytic Hydrogen Evolution. *Nano Energy* **2019**, *63*, 103849. https://doi.org/10.1016/j.nanoen.2019.06.045.

(53) Xu, J.; Zhang, C.; Liu, H.; Sun, J.; Xie, R.; Qiu, Y.; Lü, F.; Liu, Y.; Zhuo, L.; Liu, X.; Luo, J. Amorphous MoOX-Stabilized Single Platinum Atoms with Ultrahigh Mass Activity for Acidic Hydrogen Evolution. *Nano Energy* **2020**, *70*, 104529. https://doi.org/10.1016/j.nanoen.2020.104529.

(54) Yin, X.-P.; Wang, H.-J.; Tang, S.-F.; Lu, X.-L.; Shu, M.; Si, R.; Lu, T.-B. Engineering the Coordination Environment of Single-Atom Platinum Anchored on Graphdiyne for Optimizing Electrocatalytic Hydrogen Evolution. *Angew. Chem. Int. Ed.* **2018**, *57* (30), 9382–9386. https://doi.org/10.1002/anie.201804817.

(55) Ghanim, A. H.; Koonce, J. G.; Hasa, B.; Rassoolkhani, A. M.; Cheng, W.; Peate, D. W.; Lee, J.; Mubeen, S. Low-Loading of Pt Nanoparticles on 3D Carbon Foam Support for Highly Active and Stable Hydrogen Production. *Front. Chem.* **2018**, *6*, 523. https://doi.org/10.3389/fchem.2018.00523.

(56) Kunwar, D.; Zhou, S.; DeLaRiva, A.; Peterson, E. J.; Xiong, H.; Pereira-Hernández, X. I.; Purdy, S. C.; ter Veen, R.; Brongersma, H. H.; Miller, J. T.; Hashiguchi, H.; Kovarik,

L.; Lin, S.; Guo, H.; Wang, Y.; Datye, A. K. Stabilizing High Metal Loadings of Thermally Stable Platinum Single Atoms on an Industrial Catalyst Support. *ACS Catal.* **2019**, *9* (5), 3978–3990. https://doi.org/10.1021/acscatal.8b04885.

(57) Zagoraiou, E.; Daletou, M. K.; Sygellou, L.; Ballomenou, S.; Neophytides, S. G. Highly Dispersed Platinum Supported Catalysts – Effect of Properties on the Electrocatalytic Activity. *Applied Catalysis B: Environmental* **2019**, *259*, 118050. https://doi.org/10.1016/j.apcatb.2019.118050.

TOC FIGURE

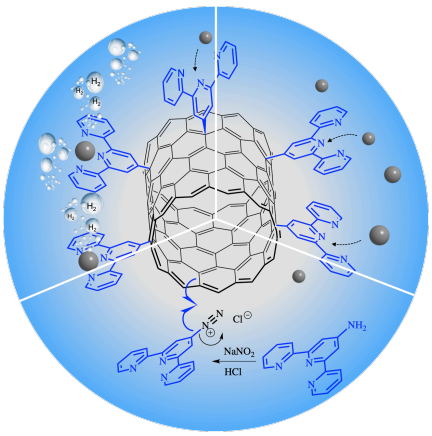

Supporting Information

"Highly Active Platinum Single-Atom Catalyst grafted onto 3D Carbon Cloth Support for the Electrocatalytic Hydrogen Evolution Reaction"

Po-Wei Yu[1], Sait Elmas[1]*, Xun Pan[1], Yanting Yin[1], Christopher T. Gibson[1,2], Gunther Andersson[1] and Mats R. Andersson[1]*

[1] - *Flinders Institute for Nanoscale Science & Technology, Flinders University, Bedford Park SA, Adelaide, Australia.*

2 - Flinders Microscopy and Microanalysis, College of Science and Engineering, Flinders University, Bedford Park, SA 5042, Australia

AUTHOR'S ORCID:

Sait Elmas: 0000-0002-1235-1436

Mats R. Andersson: 0000-0002-7928-8216

Gunther G. Andersson: 0000-0001-5742-3037

Xun Pan: 0000-0001-6087-7363

Christopher T. Gibson: 0000-0003-3334-5059

Calculating the value of Pt used in platinum single-atom catalysts on 3D carbon cloth electrode:

- Pt share price per ounce on 05.07.2021: 1107.1 US$/ounce, which is 35.59 US$/g.
- Catalyst loading in PtSAC@CC-0.5: 0.26 $\mu g \cdot cm^{-2} = 2.6 \cdot 10^{-7}$ $g \cdot cm^{-2}$
- Pt loading in PtSAC@CC-0.5 on one square meter carbon cloth: $2.6 \cdot 10^{-3}$ $g \cdot m^{-2}$
- Pt price on one square meter carbon cloth: $2.6 \cdot 10^{-3}$ $g \cdot m^{-2}$ * 35.59 US$/g = **0.10 US$•m^{-2}**
- For 20% 0.03 $mg \cdot cm^{-2}$ Pt/C the Pt loading is: $6 \cdot 10^{-6}$ $g \cdot cm^{-2}$, which amounts to **2.13 US$•m^{-2}**

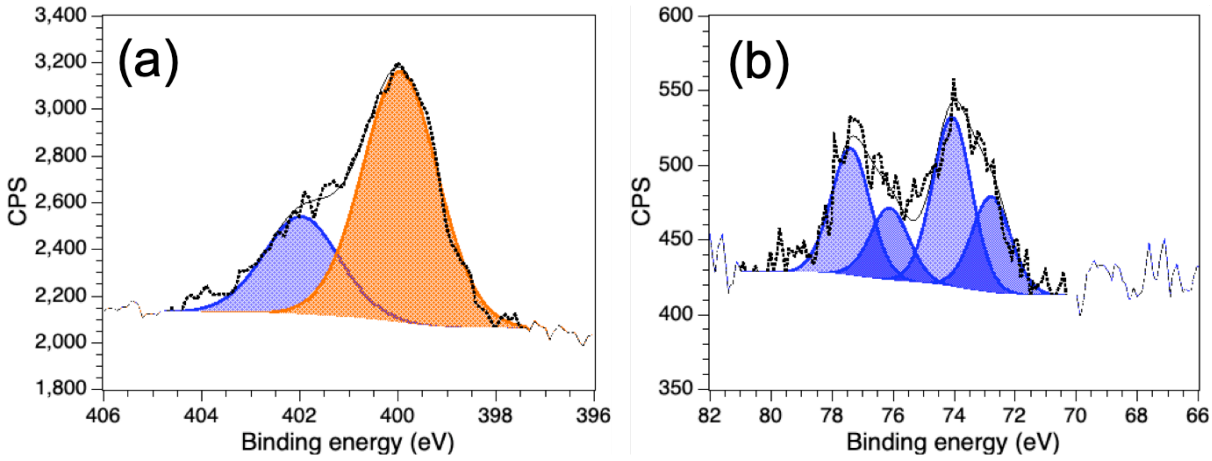

600

601 **Figure S 1:** Fitted (a) N1s and (b) Pt4f core level spectra of PtSAC-0.5 after 3 h chronoamperometric hydrogen
602 evolution reaction at 10 mA•cm^{-2} in 0.5 M H_2SO_4 using a graphite rod as counter electrode.

603

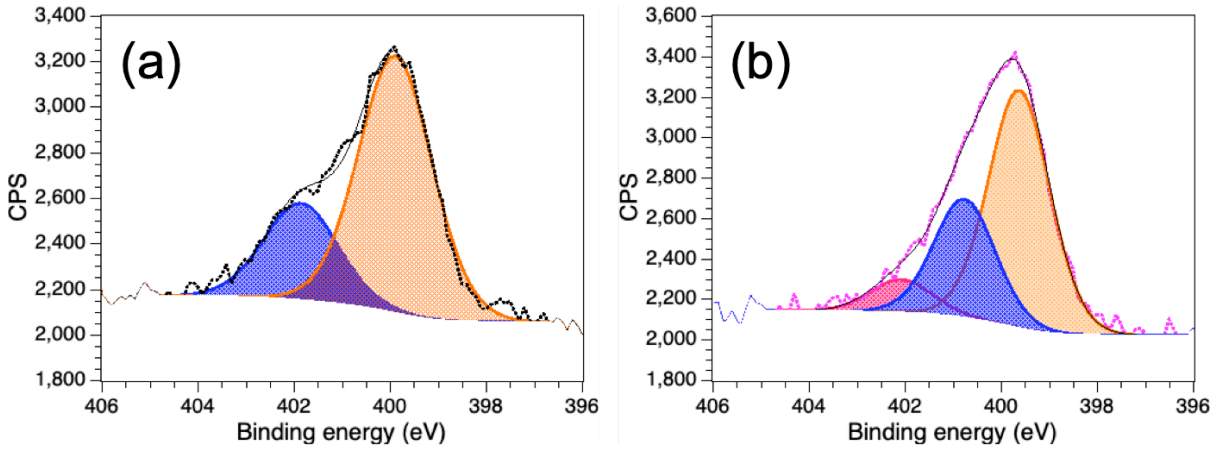

604

605 **Figure S 2:** Fitted N1s core level spectra of PtSAC-0.5 after 8 h chronoamperometric hydrogen evolution reaction at
606 10 mA•cm^{-2} in 0.5 M H_2SO_4 using a Pt wire as counter electrode before (a) and after (b) sonication for 4 minutes.

607

608

609